

Supporting Information

**Sulfur-Doping Achieves Efficient Oxygen Reduction in Pyrolyzed Zeolitic Imidazolate Frameworks**

*Chao Zhang, Bing An, Ling Yang, Binbin Wu, Wei Shi, Yu-Cheng Wang, La-Sheng Long, Cheng Wang, \*, and Wenbin Lin\**

E-mail: wangchengxmu@xmu.edu.cn, wenbinlin@uchicago.edu

## **Instrumentations and methods**

Powder X-ray diffraction (PXRD) were carried out on a Japan Rigaku DMax- $\gamma$ A rotation anode X-ray diffractometer equipped with graphite monochromatized Cu K $\alpha$  radiation ( $\lambda = 1.54 \text{ \AA}$ ). The contents of C, N, and S were quantified by Vario EL III system. The contents of Co were quantified by an inductively coupled plasma mass spectrometry (ICP-MS). The transmission electron microscopy (TEM) and EDX mapping were acquired on JEM-2010, and elemental mapping was measured on Tecnai F30 or JEM 1400 with an electron acceleration energy of 200 kV. Nitrogen sorption measurement was conducted using a Micromeritics ASAP 2020 system at 77 K. Direct current resistance tests were conducted on a Keithley 2400 Source Meter.

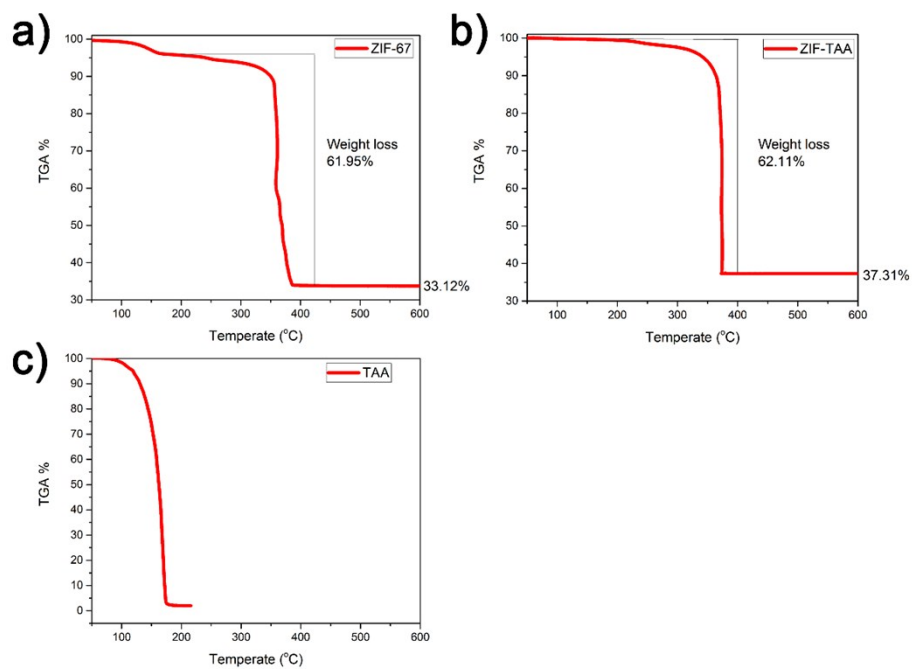


**Fig. S1.** TGA of a) ZIF-67; b) ZIF-TAA and c) TAA alone in Air atmosphere.

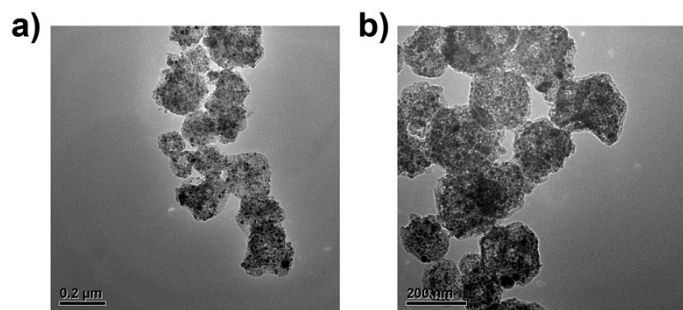


**Fig. S2.** TEM image of **ZIF-TAA-p**.

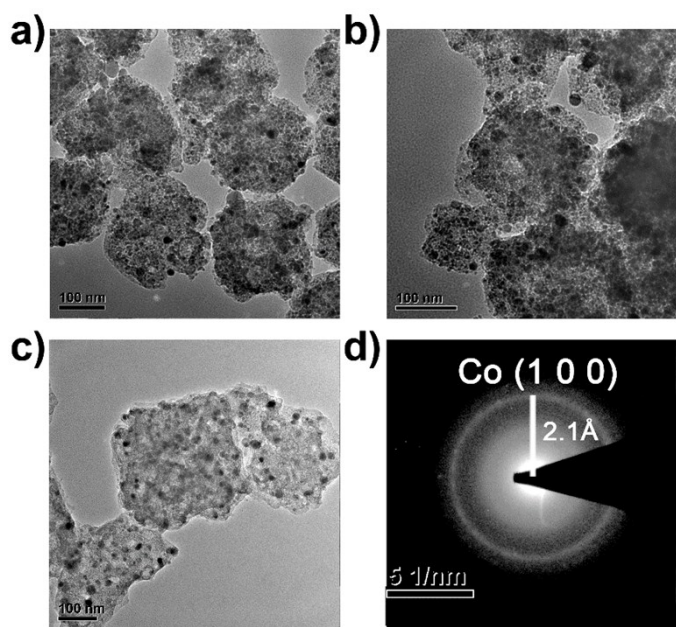


**Fig. S3.** TEM image and electron diffraction pattern of **ZIF-TAA-p** after treatment with 2 M H<sub>2</sub>SO<sub>4</sub> at room temperature for 1 hour.

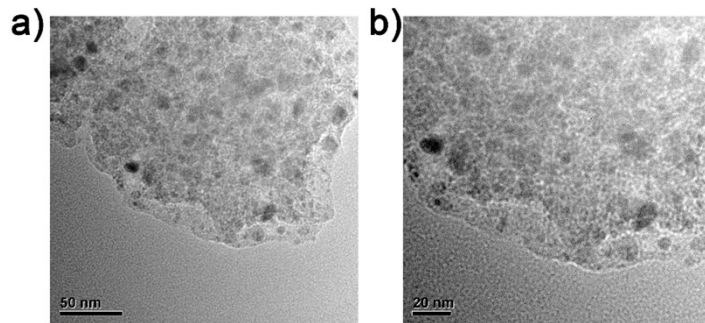


**Fig. S4.** TEM image of **ZIF-TAA-p** after hydrothermal etching in 10 M HCl at 180 °C for 24 hours.

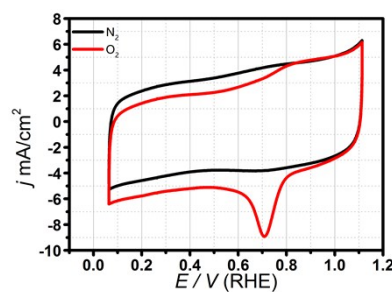


**Fig. S5.** CV curves of **ZIF-TAA-p** in  $\text{N}_2$ -saturated and  $\text{O}_2$ -saturated 0.1 M  $\text{HClO}_4$ . Scan rate: 100 mV / s.

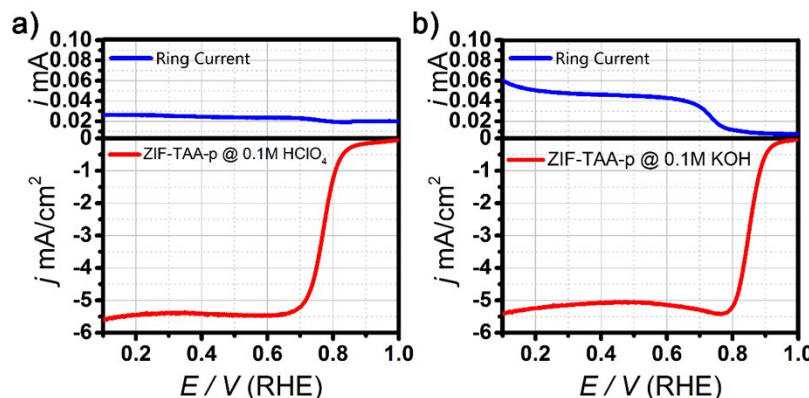


**Fig. S6.** RRDE Voltammograms of optimized **ZIF-TAA-p** in a) acid and b) alkaline media.

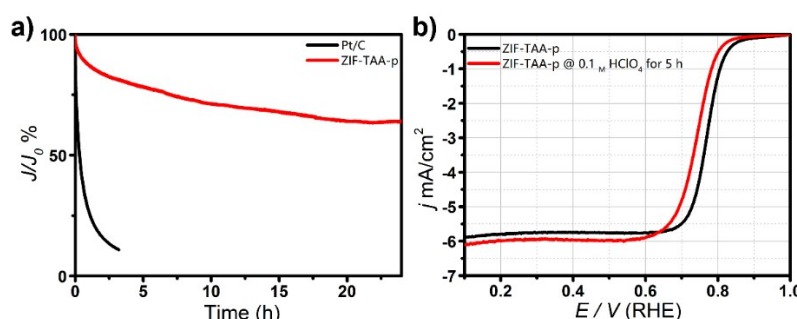


**Fig. S7.** a) Long-term durability test of **ZIF-TAA-p** and Pt/C by current-time chronoamperometry in  $\text{O}_2$ -saturated 0.1 M  $\text{HClO}_4$  (potential: 0.65V vs RHE); b) LSV comparison of **ZIF-TAA-p** and **ZIF-TAA-p** after soaking in 0.1 M  $\text{HClO}_4$  for 5 hours.

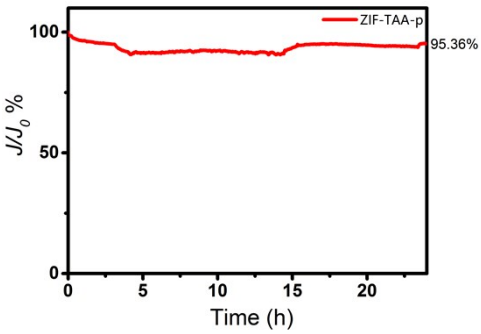


**Fig. S8.** Long-term durability test of **ZIF-TAA-p** by current-time chronoamperometry in  $O_2$ -saturated 0.1 M KOH (potential: 0.65V vs RHE).

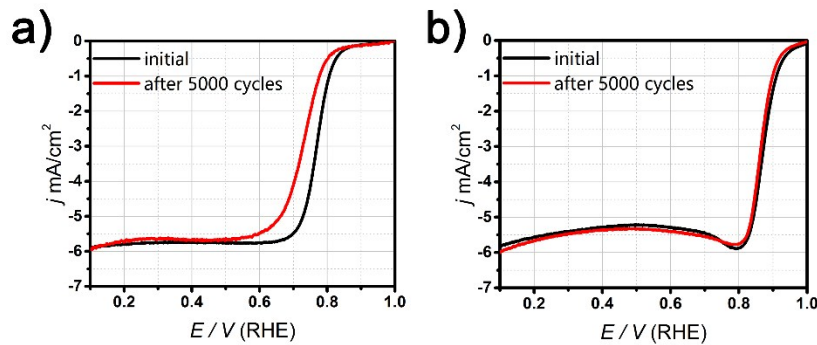


**Fig. S9.** LSV curves of **ZIF-TAA-p** before and after 5000 cycles in  $O_2$  saturated a) 0.1 M  $HClO_4$  and b) 0.1 M KOH.

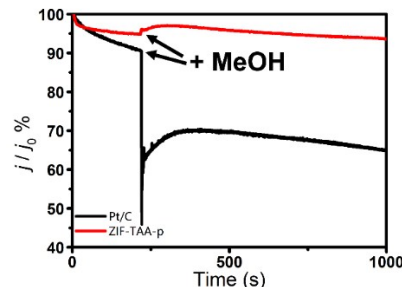


**Fig. S10.** Methanol tolerance test of **ZIF-TAA-p** and Pt/C conducted by chronoamperometry. All chronoamperometric tests were conducted at 0.65V vs RHE in  $O_2$ -saturated 0.1 M  $HClO_4$ .

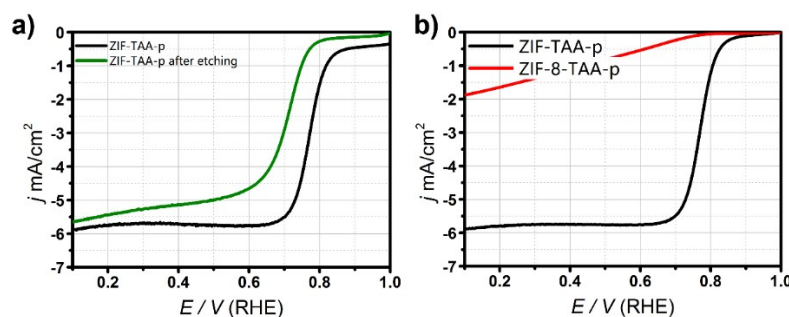


**Fig. S11.** a) LSV curves of **ZIF-TAA-p** before and after 10 M  $HCl$  etching in  $O_2$ -saturated 0.1 M  $HClO_4$ ; b) LSV curves of **ZIF-TAA-p** and pyrolyzed/sulfurated ZIF-8 (denoted as **ZIF-8-TAA-p**).

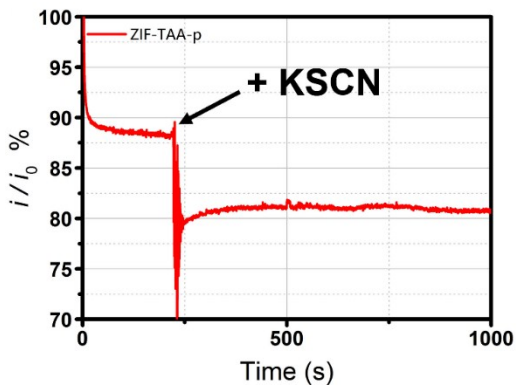


**Fig. S12.** KSCN Poisoning Experiment. Chronamperometric test of **ZIF-TAA-p** at 0.3 V in  $O_2$ -saturated 0.1 M  $HClO_4$ . The arrow indicates the introduction of KSCN.

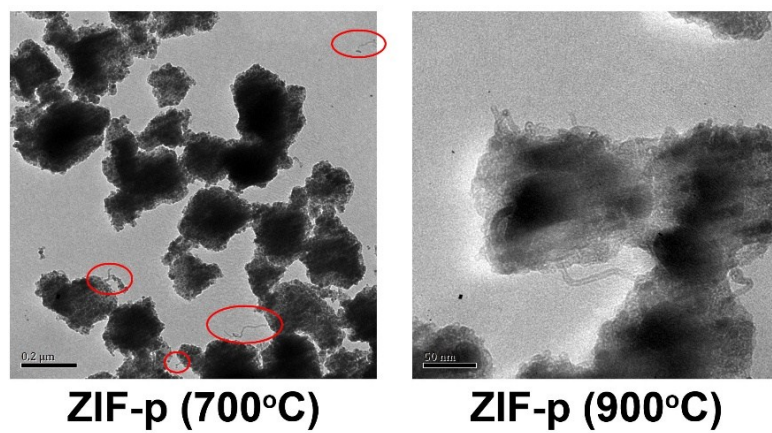


**Fig. S13.** TEM images of **ZIF-p** at different pyrolysis temperatures. The red circles on the left image point out carbon nanotubes on the external surfaces of **ZIF-p**.

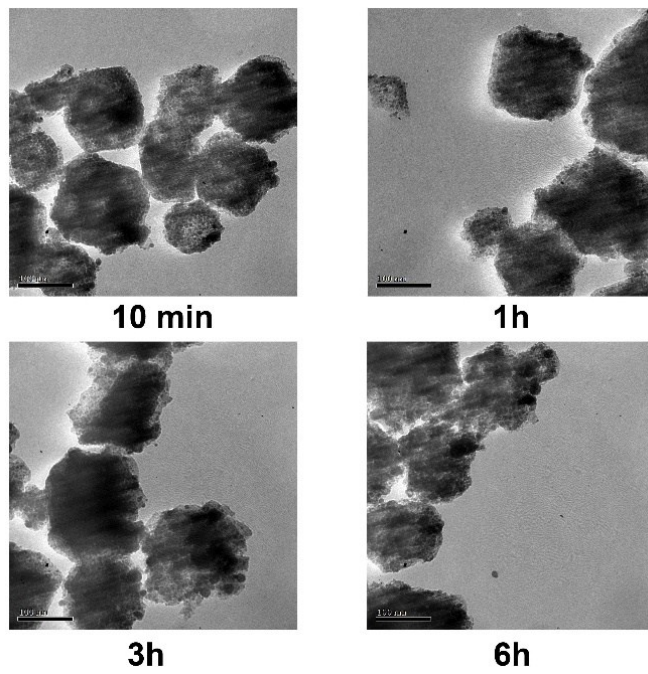


**Fig. S14.** TEM images of **ZIF-TAA-p** with different pyrolysis durations.

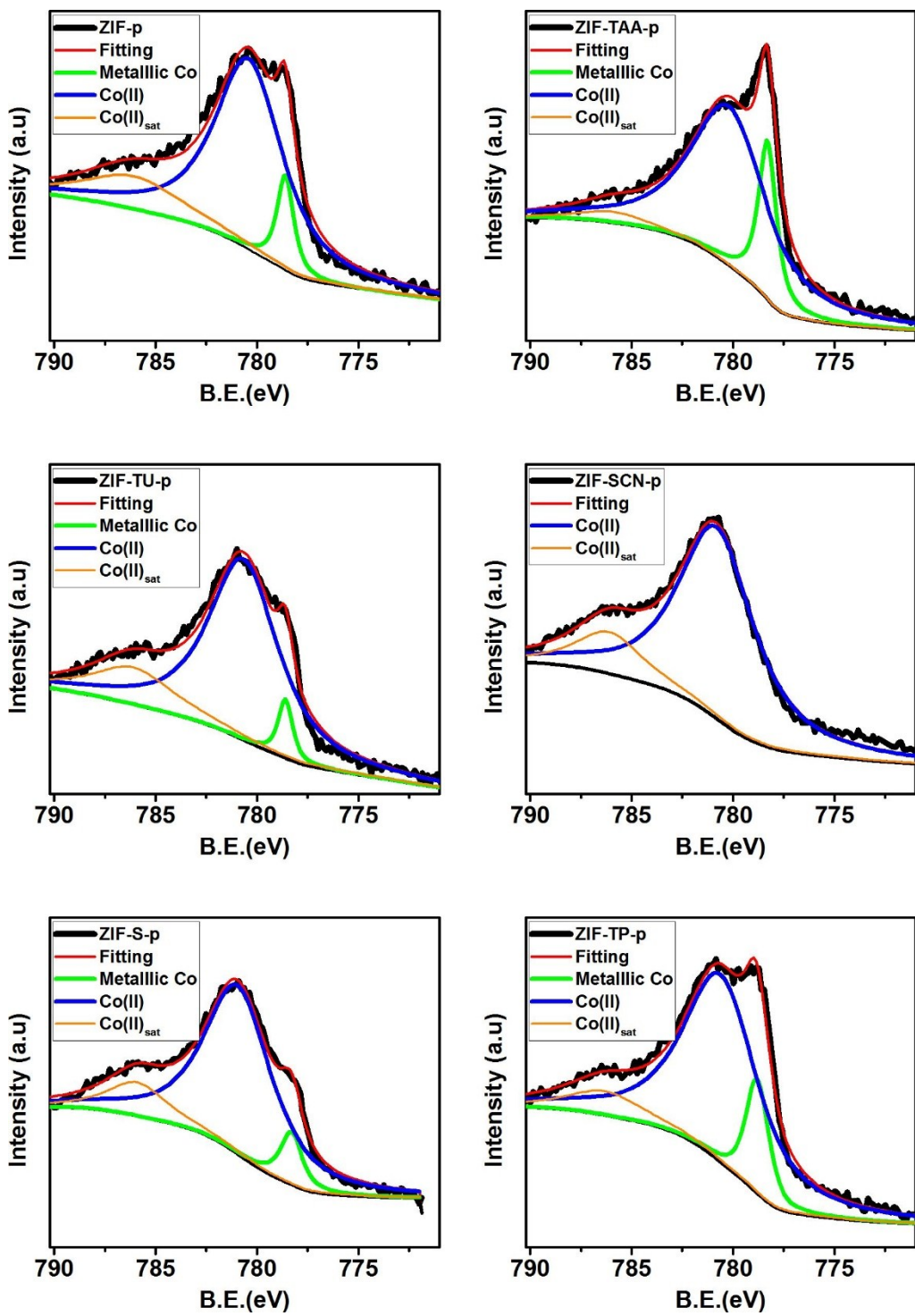
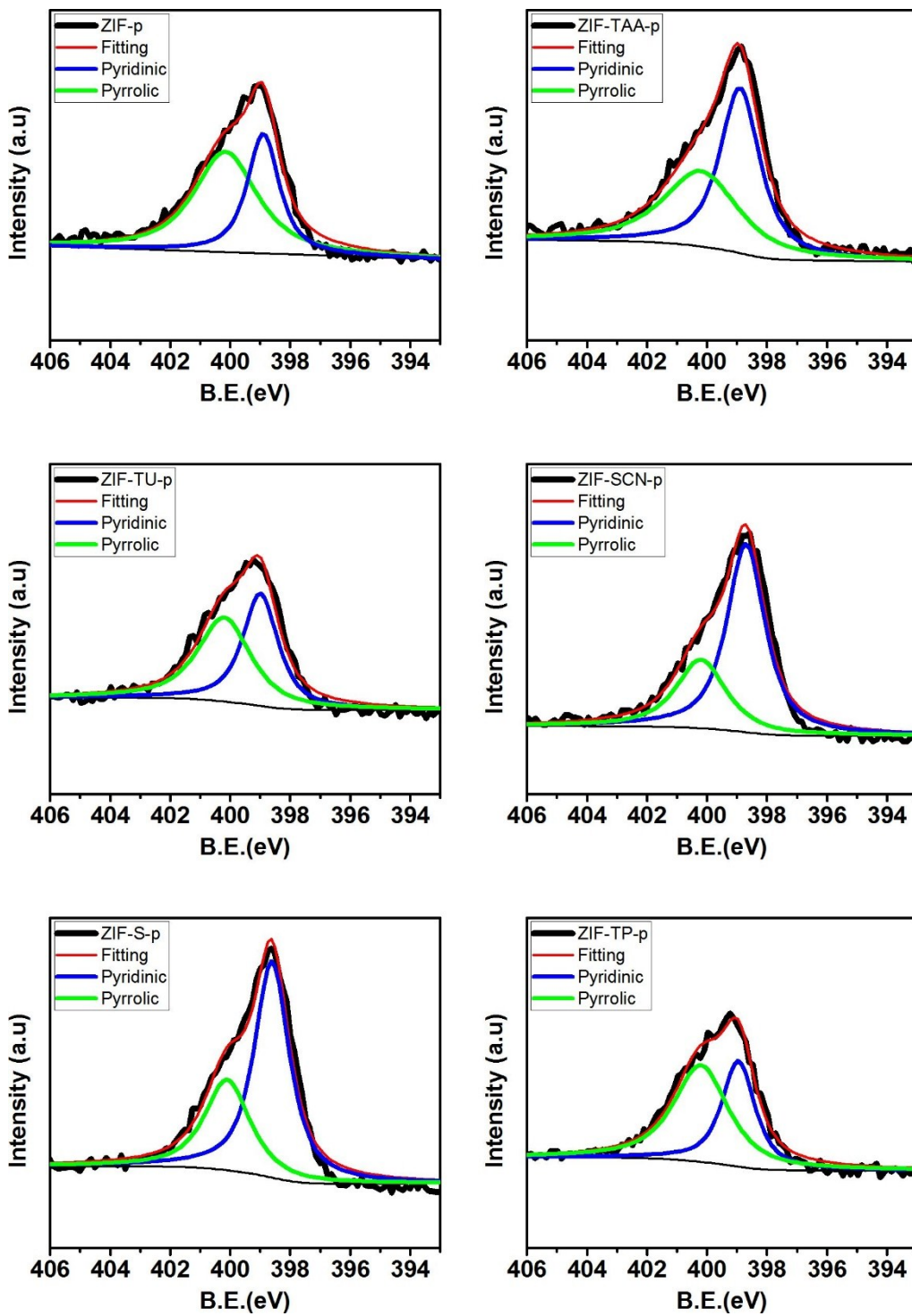


Fig. S15. XPS spectra of  $\text{Co } 2\text{p}_{3/2}$  for **ZIF-x-p**.



**Fig. S16.** XPS spectra of N 1s for **ZIF-x-p**.

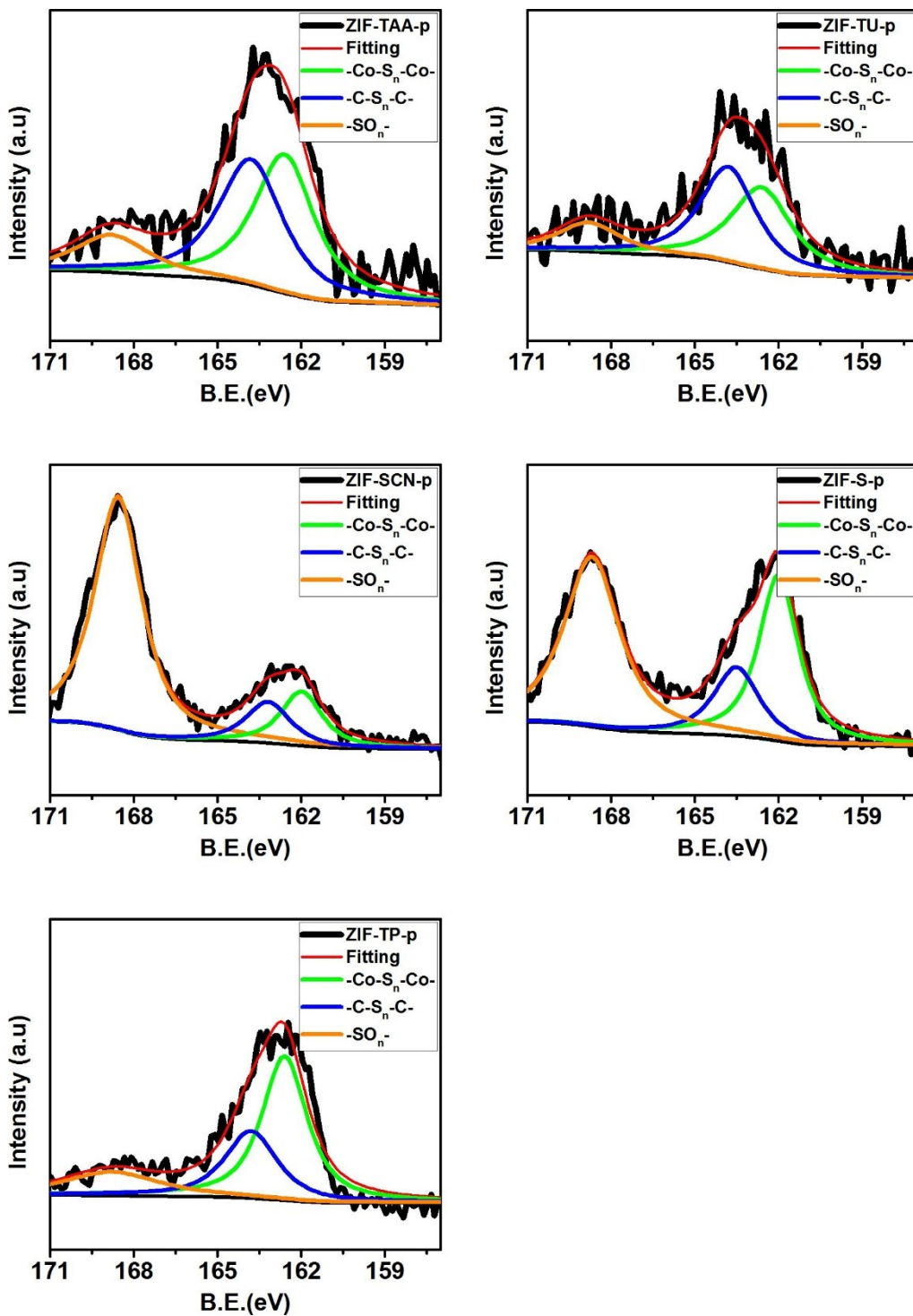
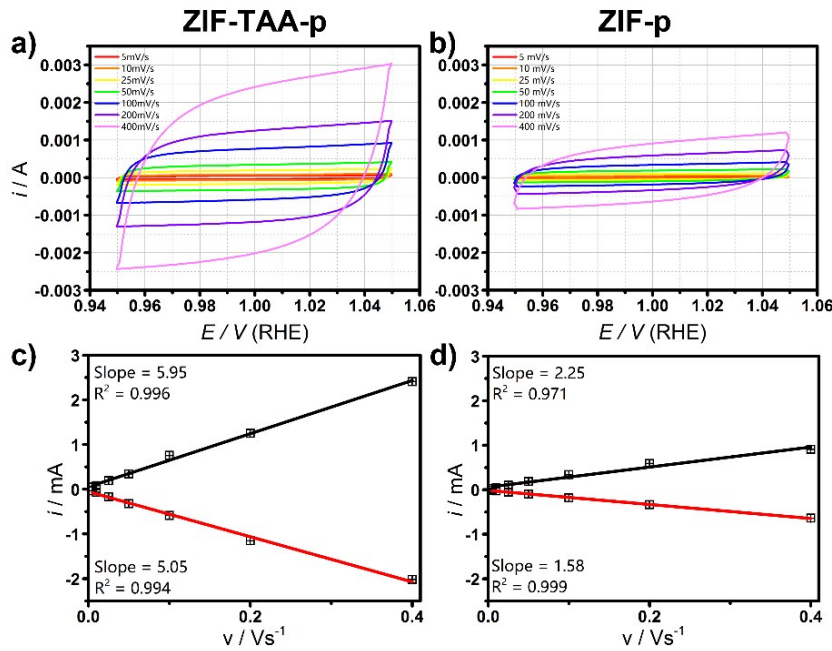
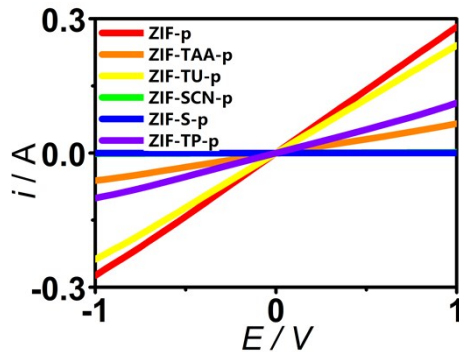


Fig. S17. XPS spectra of S 2p for ZIF-x-p.



**Fig. S18.** Charging currents measured for a) ZIF-TAA-p and b) ZIF-p in the non-Faradaic potential range of 0.95 V - 1.05 V at scan rates of 5, 10, 25, 50, 100, 200, and 400 mV / s, respectively. c) and d) are corresponding cathodic and anodic charging currents measured at 0 V, plotted against the scan rates. The double-layer capacitance is calculated from the average of the absolute value of anodic and cathodic slopes and the catalysts loading (0.1 mg).



**Fig. S19.** Direct current I/V plots of ZIF-x-p.

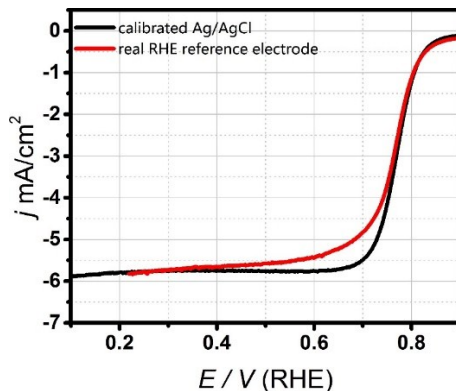


**Fig. S20.** The comparison of a calibrated Ag/AgCl reference electrode and a RHE reference electrode in 0.1 M HClO<sub>4</sub>.

**Table S1.** Comparison of ORR catalytic performances in acid media (electrolyte is 0.1 M HClO<sub>4</sub> and rotating speed is 1600 rpm if not marked).

Catalyst	Oneset Potential (V vs RHE)	Half-wave potential (V vs RHE)	diffusion-limited current density at 0.4 V (mA / cm <sup>2</sup> , rotating speed 1600 rpm)	Refs
ZIF-TAA-p	0.88	0.78	5.8	This work
CoIM	0.83	0.68	4	[S1]
FeIM/ZIF-8	0.915	0.755	5	[S2]
Zn(eIm) <sub>2</sub> TPIP	0.914	0.78	5	[S3]
ZIF-67-900-AL	0.85	0.71	4	[S4]
MDC	0.86	0.71	5.2	[S5]
C-N-Co <sup>a</sup>	0.87	0.79	4.8	[S6]
PFeTTPP-1000	0.93	0.76	5	[S7]
Fe/N/C-SCN <sup>b</sup>	0.91	0.836	4.1 <sup>c</sup>	[S8]
CPANIFe-NaCl	0.91	0.72	5.1	[S9]
PNGF	0.83	0.67	7.5	[S10]

<sup>a</sup> Electrolyte: 0.5 M H<sub>2</sub>SO<sub>4</sub>

<sup>b</sup> Electrolyte: 0.1 M H<sub>2</sub>SO<sub>4</sub>

<sup>c</sup> Rotating speed: 900 rpm

**Table S2.** Comparison of ORR catalytic performances in alkaline media (electrolyte is 0.1 M KOH and rotating speed is 1600 rpm if not marked).

Catalyst	Oneset Potential (V vs RHE)	Half-wave potential (V vs RHE)	diffusion-limited current density at 0.4 V (mA / cm <sup>2</sup> , rotating speed 1600 rpm)	Refs
ZIF-TAA-p	0.98	0.88	5.3	This work
ZIF-67-900-AL	0.92	0.85	5.2	[S4]
P-CNCo-20	0.93	0.85	6	[S11]
Fe-N/C-800	0.98	0.81	4.8	[S12]
N/Co-doped PCP-RGO	0.94	0.87	7.2	[S13]
GNPCSSs-800	0.957	0.786	6	[S14]
Co/C-700	0.81	0.86	4	[S15]
PNGF	1.03	0.86	7	[S10]
MIL-800	0.91	0.79	4.8	[S16]

**Table S3** C, N and S contents of **ZIF-x-p<sup>a</sup>**

Sample	content %		
	C	N	S
ZIF-TAA	38.22±0.70	27.47±0.62	1.16±0.24
ZIF-TAA-p (10 min)	39.76 ± 0.86	9.91 ± 0.54	1.57 ± 0.14
ZIF-TAA-p (3 hour)	40.59 ± 1.24	7.23 ± 0.31	1.32 ± 0.14
ZIF-TAA-p (6 hour)	32.74 ± 1.21	4.85 ± 0.37	1.20 ± 0.11
ZIF-TU-p	40.33 ± 2.02	6.50 ± 0.30	0.64 ± 0.21
ZIF-SCN-p	28.31 ± 0.54	11.00 ± 0.20	7.17 ± 0.40
ZIF-S-p	30.61 ± 1.85	14.63 ± 0.63	5.12 ± 0.07
ZIF-TP-p	42.68 ± 2.07	6.69 ± 0.39	0.41 ± 0.08
ZIF-p	41.46 ± 0.23	6.7.0 ± 0.11	-

<sup>a</sup> The pyrolysis temperature was 700 °C under Ar, and the pyrolysis duration was 10 minutes if not marked.

**Table S4** Relative Co species contents with respect to total Co of **ZIF-x-p** based on XPS

Sample	Co(0)	Co(II)
ZIF-p	11.05%	88.95%
ZIF-TAA-p	19.36%	80.64%
ZIF-TU-P	6.25%	93.75%
ZIF-SCN-P	0.00%	100.00%
ZIF-S-p	9.25%	90.75%
ZIF-TP-p	14.75%	85.25%

**Table S5** Relative pyridinic N contents with respect to total N of **ZIF-x-p** based on XPS

Sample	pyridinic N
ZIF-p	37.64%
ZIF-TAA-p	53.26%
ZIF-TU-P	47.25%
ZIF-SCN-P	67.97%
ZIF-S-p	34.88%
ZIF-TP-p	39.86%

**Table S6** Relative S species contents with respect to total S of **ZIF-x-p** based on XPS

Sample	-SO <sub>n</sub> -	C-S <sub>n</sub> -C	Co-S <sub>n</sub> -Co
ZIF-TAA-p	14.48%	41.99%	43.53%
ZIF-TU-P	15.07%	44.01%	40.92%
ZIF-SCN-P	73.15%	12.09%	14.76%
ZIF-S-p	49.25%	16.37%	34.38%
ZIF-TP-p	18.54%	28.48%	52.98%

**Table S7** Resistance measurement data of **ZIF-x-p**

Sample	Slope	S/L <sup>a</sup>	Resistivity
ZIF-TAA-p	0.0633	9.648	152.41706
ZIF-TU-p	0.24132	26.10692	108.18384
ZIF-SCN-p	0.00145	13.91508	9596.60825
ZIF-S-p	5.52865E-5	3.85932	69805.80816
ZIF-TP-p	0.10613	11.46981	108.07443
ZIF-p	0.28026	13.71198	48.92591

<sup>a</sup> S: Areas of conductive adhesive; L: Thicknesses of tablets

## References

- [S1] S. Ma, G. A. Goenaga, A. V. Call, D.-J. Liu, *Chem. – Eur. J.* **2011**, *17*, 2063.
- [S2] D. Zhao, J.-L. Shui, C. Chen, X. Chen, B. M. Reprogole, D. Wang, D.-J. Liu, *Chem. Sci.* **2012**, *3*, 3200.
- [S3] D. Zhao, J.-L. Shui, L. R. Grabstanowicz, C. Chen, S. M. Commet, T. Xu, J. Lu, D.-J. Liu, *Adv. Mater.* **2014**, *26*, 1093.
- [S4] X. Wang, J. Zhou, H. Fu, W. Li, X. Fan, G. Xin, J. Zheng, X. Li, *J. Mater. Chem. A* **2014**, *2*, 14064.
- [S5] W. Xia, J. Zhu, W. Guo, L. An, D. Xia, R. Zou, *J. Mater. Chem. A* **2014**, *2*, 11606.
- [S6] H.-W. Liang, W. Wei, Z.-S. Wu, X. Feng, K. Müllen, *J. Am. Chem. Soc.* **2013**, *135*, 16002.
- [S7] S. Yuan, J.-L. Shui, L. Grabstanowicz, C. Chen, S. Commet, B. Reprogole, T. Xu, L. Yu, D.-J. Liu, *Angew. Chem.* **2013**, *125*, 8507.
- [S8] Y.-C. Wang, Y.-J. Lai, L. Song, Z.-Y. Zhou, J.-G. Liu, Q. Wang, X.-D. Yang, C. Chen, W. Shi, Y.-P. Zheng, M. Rauf, S.-G. Sun, *Angew. Chem. Int. Ed.* **2015**, 9907.
- [S9] W. Ding, L. Li, K. Xiong, Y. Wang, W. Li, Y. Nie, S. Chen, X. Qi, Z. Wei, *J. Am. Chem. Soc.* **2015**, *137*, 5414.
- [S10] X. Zhou, Z. Bai, M. Wu, J. Qiao, Z. Chen, *J. Mater. Chem. A* **2015**, *3*, 3343.

- [S11] Y.-Z. Chen, C. Wang, Z.-Y. Wu, Y. Xiong, Q. Xu, S.-H. Yu, H.-L. Jiang, *Adv. Mater.* **2015**, 5010.
- [S12] W. Niu, L. Li, X. Liu, N. Wang, J. Liu, W. Zhou, Z. Tang, S. Chen, *J. Am. Chem. Soc.* **2015**, 137, 5555.
- [S13] Y. Hou, Z. Wen, S. Cui, S. Ci, S. Mao, J. Chen, *Adv. Funct. Mater.* **2015**, 25, 872.
- [S14] H. Zhong, J. Wang, Y. Zhang, W. Xu, W. Xing, D. Xu, Y. Zhang, X. Zhang, *Angew. Chem. Int. Ed.* **2014**, 53, 14235.
- [S15] A. Kong, C. Mao, Q. Lin, X. Wei, X. Bu, P. Feng, *Dalton Trans.* **2015**, 44, 6748.
- [S16] C. Mao, A. Kong, Y. Wang, X. Bu, P. Feng, *Nanoscale* **2015**, 7, 10817.